

# ENERGY TRANSFER AS A PROBE OF PROTEIN DYNAMICS IN THE PROTEINS TRANSFERRIN AND CALMODULIN

PATRICIA B. O'HARA, KATHLEEN M. GORSKI, AND MARK A. ROSEN  
*Department of Chemistry, Amherst College, Amherst, Massachusetts 01002*

**ABSTRACT** We have initiated an investigation into the usefulness of fluorescence energy transfer in probing protein dynamics. Our analysis involves measuring the energy transfer efficiency while perturbing the protein conformational equilibrium with heat. As the temperature increases, the amplitudes of vibrations increase, and fluorescence energy transfer should also increase if the donor and acceptor are in a flexible region of the protein. A theoretical analysis developed by Somogyi and co-workers for the temperature dependence of dipole-dipole energy transfer (Somogyi, B., J. Matko, S. Papp, J. Hevessey, G. R. Welch, and S. Damjanovich. 1984. *Biochemistry*. 23:3403-3411) was tested by the authors in one protein system. Energy transfer from tryptophan to a pyridoxamine derivatized side group in RNase increased 40% over 25°C. Here we report further testing of this model in two additional protein systems: calmodulin, a calcium activated regulatory protein, and transferrin, a blood serum iron shuttle. Our studies show a slight differential sensitivity of the transfer efficiency to heat for the two systems. Normalized energy transfer over 6.5 Å in calmodulin from a tyrosine donor to a Tb(III) acceptor increases 40% from 295 to 320 K. Normalized energy transfer over 42 Å in transferrin from a Tb(III) donor to an Fe(III) acceptor increases 35% over the same temperature range. Whereas these results demonstrate that thermally induced fluctuations do increase energy transfer as predicted by Somogyi, they also appear rather insensitive to the nature of the protein host environment. In contrast to the Förster processes examined above, energy transfer over very short distances has shown an anomalously high temperature dependence.

## INTRODUCTION

Förster Energy Transfer (FET), the transfer of energy from a donor to an acceptor via a dipole-dipole mechanism, has long been used to measure distances between a donor and an acceptor in proteins and other macromolecules (1). Here we report an investigation into the use of the thermal profile of FET to probe fluctuations in donor-acceptor distances that result from the intrinsic dynamics of the system. The thermal profile of FET tests the rigidity of a macromolecule and is an indirect method of investigation of both local and global vibrational modes. With the proper selection of donor, acceptor, and macromolecular environment, different types of motions can be sampled.

The theoretical background for this analysis, developed by Somogyi and co-workers (2), introduces a "normalized" energy transfer parameter,  $f$ . This normalization takes into account the temperature dependence of all of the other pathways that contribute to deactivation of an excited state. If the observed quenching efficiency is interpreted as

an average over the multiple conformational states that the system samples over the lifetime of the donor-excited state, then changes in this parameter give indirect structural information. Heat added to a macromolecule causes greater population of excited vibrational modes, characterized by larger vibrational amplitudes. Thus, though the equilibrium donor-acceptor distance may remain the same, the shortest distance between the two will decrease. Because FET depends upon the inverse sixth power of the donor-acceptor distance, these small distance fluctuations can result in large perturbations in the transfer efficiency. The distance measured by FET may become increasingly weighted towards this shortest distance as the temperature increases. Both the measured energy transfer efficiencies and the calculated distances will depend on the relative rate constants for the decay of the intrinsic donor fluorescence and for motions contributing to deactivation. In a rigid structure, the normalized energy transfer parameter,  $f$ , will not be a sensitive function of temperature. If donor and acceptor are in a less rigid region of the macromolecule, the normalized FET may be very sensitive to temperature. Therefore, analysis of the sensitivity of  $f$  to temperature should provide information as to the dynamics relevant to a particular donor-acceptor domain in a protein.

Somogyi tested his model using energy transfer from

Address reprint requests to Patricia B. O'Hara.

A preliminary account of this work was presented at the International Symposium on Quantitative Luminescence Spectrometry in Biomedical Sciences in May, 1987, the proceedings of which will soon be published in the journal, *Anal. Chim. Acta*.

tryptophan to pyridoxamine monophosphate (PMP) in RNase. His theoretical model is examined here in two additional donor-acceptor environments, human serum transferrin and bovine brain calmodulin. Energy is transferred over 42 Å in the Fe(III) transport protein transferrin (Tf) from a Tb(III) donor at one of the two metal binding sites, to an Fe(III) acceptor at the other metal binding site (3). These two metal binding sites are in different domains of the protein separated by ~42 Å (4). The thermal profile and normalized FET that we have measured are consistent with the theoretical model just described and show an increased energy transfer with temperature. In a second system, energy transfer occurs over ~6.5 Å in the regulatory protein calmodulin (CaM) (5). Here the donor is Tyr 99 and the acceptor is Tb(III) substituted for Ca(II) in one of the Ca(II) binding loops. Again we find agreement with the theoretical model, an increase in the normalized energy transfer with temperature. The relative increases for these three protein environments, RNase, CaM, and Tf, are compared in terms of the known protein structures.

We have also examined the temperature dependence of energy transfer, again in Tf, but now from a donor, Tyr, bound directly to a Tb(III) acceptor. The proximity of donor and acceptor precludes the simple application of Förster theory in this system. In contrast to the three systems above, this system has an unusually high temperature dependence. Apparently, the short-range mechanisms of energy transfer active in this system, are much more temperature dependent than Förster transfer.

Our analysis has been facilitated and simplified by the use of the highly luminescent lanthanide, Tb(III), which substitutes for the natural metal, Fe(III) in Tf and Ca(II) in CaM. These measurements are facilitated by using Tb(III) because, as a donor, it has an extremely long lifetime (1.2 ms in Tb-Tf) during which it is free to sample even very slow conformational fluctuations which may be inaccessible by other dynamic probes. Energy transfer measurements using lanthanides are also simplified due to the fact that the electronic transition dipole moment is essentially isotropic. Therefore, uncertainties due to changes in the relative orientations of the donor and acceptor transition dipole moments, ( $\kappa^2$  in Förster theory), are very small, and the averaged value of  $\frac{2}{3}$  for  $\kappa^2$  is a good approximation. The full range of values for  $\kappa^2$  in cases where a lanthanide is used as a donor or an acceptor and a nonisotropic species is used as the second half of the donor-acceptor pair is narrowed from 0–4 (the range for two nonisotropic donors) to 0.33–1.31 (1), which makes the error in distance arising from uncertainties in  $\kappa^2$  at most 8.8%. An additional advantage is that as an acceptor, the Tb(III) 550-nm luminescent intensity can be used to indirectly calculate the efficiency of donor quenching when difficulties measuring the donor fluorescent intensity arise due to low sensitivity. Because Tb(III) may also bind to low-affinity nonspecific sites on proteins, its use is limited

to those systems that contain a high-affinity metal binding site into which it can be substituted.

## EXPERIMENTAL METHODS

### Fluorescence Measurements

All of the fluorescence and luminescence data were measured using a Fluorometer (Spex Industries, Edison, NJ) with a single excitation monochromator and a double emission monochromator. Excitation and emission slits were 0.25 and 0.5 mm for the Tf experiments and 0.5 and 1.0 mm for the CaM experiments. The data were corrected for fluctuations in the light intensity and for photomultiplier response. In the case of calmodulin, the signal was also corrected for the interfering water raman signal.

The sample compartments were thermostatted with circulating water using a temperature bath (Lauda Div., Brinkmann Instruments Co., Westbury, NY). The temperature of the water bath was raised or lowered with a 30-min wait at each new setting to insure thermal equilibration. Before use, all protein samples were equilibrated with metal for at least 30 min at room temperature, filtered with a 1.2 µm filter, and degassed by flushing with nitrogen.

### Transferrin

Human serum transferrin, 99% metal free (apoTf), was purchased from Sigma Chemical Co., St. Louis, MO, and dialyzed extensively before use to remove excess chelates. The concentrations of apoTf solutions were measured spectrophotometrically using an extinction coefficient  $\epsilon_{280} = 89,600 \text{ M}^{-1}\text{cm}^{-1}$  (6). Buffer solutions contained 10 mM NaHCO<sub>3</sub>, and 25 mM of either Hepes or MOPS, pH 8.0. A slightly alkaline pH insures the specificity of binding of the lanthanide by Tf as judged by optical criteria (7). Bicarbonate is a requisite anion for Fe(III) binding to Tf. Tb(III) not specifically bound to the metal binding site in the Tf in this buffer at these concentrations provides no background.

**Terbium-Transferrin (Tb<sub>2</sub>-Tf).** Terbium chloride (TbCl<sub>3</sub>·6H<sub>2</sub>O) was purchased from Alfa Products, Danver, MA, and vacuum desiccated before use. Tb<sub>2</sub>-Tf was prepared by adding aliquots of 10 mM Tb(III) stock to a solution of apoTf in buffer. Different concentrations were used in various experiments. Typical concentrations for direct Tb(III) excitation were 66 µM Tb(III), 33 µM Tf. Typical concentrations for indirect Tb(III) excitation were 18 µM Tb(III), 10 µM Tf. The higher concentrations for direct excitation are necessary due to the very small extinction coefficients for Tb(III). Samples were excited either directly at 502 nm or indirectly at 295 nm. The emission was collected from either 510–600 nm or 300–600 nm.

**Iron-Terbium-Transferrin.** Fe(III) was specifically loaded into site A of Tf by adding Fe(III)-nitrilotriacetate to the apoprotein at low pH, slowly raising the pH to 7.0, and then dialyzing away the nitrilotriacetate chelate in the presence of bicarbonate (8). The B site of Tf can then be loaded with Tb(III), which is added to the Fe-Tf as just described. This elaborate procedure insures that each Tb(III) donor has a companion Fe(III) acceptor to quench it. Excitation and emission parameters were the same as for Tb-Tf. Typical concentrations were 100 µM in Tb(III), Fe(III), and Tf.

### Calmodulin

Calmodulin (CaM) was isolated from bovine brain by phenyl Sepharose affinity chromatography by the method of Gopalakrishna and Anderson (9), and its activity tested by the ability to activate CaM-deficient phosphodiesterase (10). All CaM fluorescence experiments utilized a buffer of either 25 mM Hepes, 0.1 M KCl, at pH 7.0, buffer A, or 25 mM Hepes, 0.1 M KCl, 10 mM NaHCO<sub>3</sub>, pH 8.0, buffer B. CaM concentrations were determined spectrophotometrically using  $\epsilon_{278} = 3006 \text{ M}^{-1}\text{cm}^{-1}$ . All glassware was acid washed to prevent extraneous contamination by Ca(II) and all buffers were chelexed before use. CaM

fluorescence emission spectra must be corrected for the water raman signal which interferes with the fluorescence intensity measurement at 308 nm under the conditions of the experiments.

**Ca-CaM.** Solutions were typically 39.5  $\mu\text{M}$  in CaM and 1.25 mM in Ca(II) in buffer to insure complete saturation with Ca(II). At full saturation, the bound metal-to-protein ratio is 4:1, for a metal to binding site ratio of 1:1. Fluorescence experiments using a 278-nm excitation wavelength were characterized by a fluorescence peak at 308 nm assigned to Tyr 99 (CaM contains no Trp).

**Tb-CaM.** 10 mM Tb(III) stock solutions were made as just described. Solutions were  $\sim 40.0 \mu\text{M}$  in CaM. Tb(III) was added to the protein either at a slight excess, Tb(III) = 200 mM, buffer A, or large excess, Tb(III) = 1.0 mM, buffer B, to insure complete protein saturation. Fluorescence experiments using a 278-nm excitation wavelength were characterized by a diminished protein fluorescence peak at 308 nm and a new peak at 550 nm arising from energy transfer to Tb(III) and subsequent emission. The indirect mode of excitation and the buffers and pH used in each experiment all insured that only Tb(III) bound to the specific sites was observed. Under these conditions, Tb(III) not bound to the protein has no measurable fluorescence.

## RESULTS AND ANALYSIS

### Analysis of Energy Transfer

The rate constant for dipole-dipole energy transfer,  $k_t$ , is dependent on the inverse sixth power of the donor-acceptor distance,  $R$  (11).

$$k_t = (d J n^{-4} \kappa^2) k_f R^{-6} = C k_f R^{-6}.$$

Here  $d$  is a unit dependent constant,  $J$  is the spectral overlap integral,  $n$  is the index of refraction, and  $\kappa$  represents a measure of the relative orientation of the donor and acceptor transition dipole moments. Because  $d$ ,  $J$ ,  $n$  and  $\kappa^2$  are unique constants in each of our systems, they can be represented by a system-dependent constant,  $C$ .  $k_f$  is the rate constant for fluorescence. The efficiency of energy transfer,  $E$ , can be expressed as the ratio of the transfer rate constant to the sum of all the rate constants for deactivation of the excited state.

$$E = [k_t / (k_t + k_i + k_o)],$$

where  $k_o$  represents the sum of the rate constants for all of the other processes for deactivation.  $E$  can be experimentally measured from either time-resolved data or steady-state data.

$$E = (1 - \tau_{DA}/\tau_D) = (1 - F_{DA}/F_D),$$

where  $\tau$ 's are the lifetimes and  $F$ 's are fluorescence intensities of the donor, D, and the donor-acceptor, DA, respectively.

If we now consider small fluctuations,  $r$ , which can occur about the equilibrium distance  $R(r = 0)$ , then the measured system transfer rate constant and calculated DA distance can be expressed as follows.

$$\langle k_t(r) \rangle = C k_f \langle R(r)^{-6} \rangle,$$

and the corresponding efficiencies are.

$$\langle E \rangle = \langle (1 - \tau_{DA}/\tau_D) \rangle = \langle (1 - F_{DA}/F_D) \rangle.$$

Fig. 1 illustrates how the averaged transfer rate constant will depend on the relative sizes of  $r$  and  $R(0)$  for a static system in which the fluctuation is slow compared with the rate constant for deactivation of the excited state, so averaging becomes an arithmetic average over the two states. As an example, consider a small-scale fluctuation of 0.10 Å in a system where  $R(0)$  is 5.0 Å. This perturbation is reflected in a 1.01-fold increase in the averaged transfer rate constant. The distance  $\langle R \rangle$  derived from such a measurement would be only slightly less than  $R(0)$  ( $\langle R \rangle = 4.99 \text{ Å}$ ). Thus, if a system is structurally rigid, increasing the temperature will not produce a significant increase in the vibrational amplitude, and the measured rate constant and calculated energy transfer efficiency and distance will be only slightly sensitive, if at all, to the increased temperature. Now consider a system with greater flexibility. In this system, a 1.0-Å fluctuation in a  $R(0)$  of 5.0 Å would result in a 2.07-fold enhancement of the averaged transfer rate constant. The distance calculated here would be much less than  $R(0)$  ( $\langle R \rangle = 4.43 \text{ Å}$ ). This effect becomes more dramatic as the fluctuation gets larger. Remember that this example represents an extreme case in which the macromolecule is frozen during energy transfer. The opposite extreme case would be one where all possible D-A distances are sampled during the excited state lifetime. Measurements such as  $\langle R \rangle$  and  $\langle E \rangle$  derived from these dynamic systems are also system averages and are sensitive to temperature, though averaging is done in a different manner.

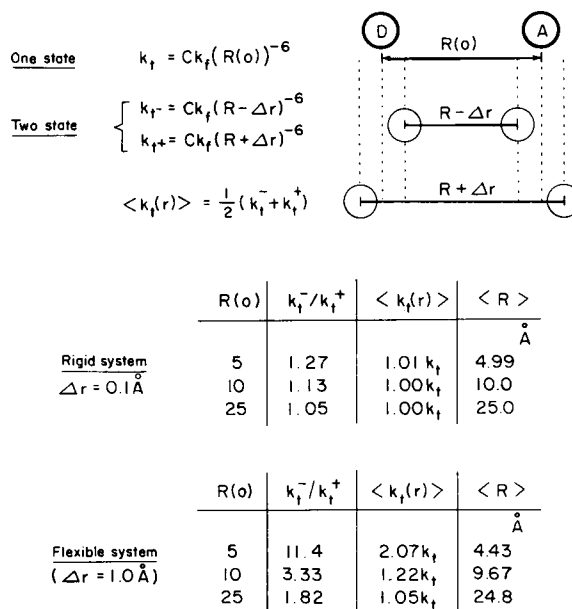


**FIGURE 1** Analysis of the results of static averaging in a two-state system. Upper part shows a model for a donor, D, and acceptor, A, separated a distance  $R(0)$  from one another. Fluctuations can occur in the donor-acceptor distances. The two sets of numbers represent the two-state system undergoing small fluctuations (rigid system), and large fluctuations (flexible system).  $k_t$  is the energy transfer rate constant,  $C$  is a constant defined in the text, and  $k_f$  is the fluorescent rate constant.

TABLE I  
THERMAL PROFILES OF NORMALIZED  
ENERGY TRANSFER

I. Energy transfer from Trp to pyridoxamine monophosphate in RNase*					
T (K)	293.0	298.0	306.0	310.0	314.0
$f'$ (%)	100	103	114	127	138
II. Energy transfer from Tb(III) to Fe(III) in transferrin (direct excitation)					
T (K)	296.0	309.2	319.0		
$f'$ (%)	100	123	132		
III. Energy transfer from Tyr to Tb(III) in bovine brain calmodulin					
T (K)	283.0	293.0	303.0	313.0	333.0
$f'$ (%)	89	100	111	128	164

\*Calculated from data in reference 2.

Somogyi's method of analyzing changes in local fluctuations of a protein matrix by FET requires the measurement of either the lifetime or fluorescence intensity of the donor in the presence and absence of an acceptor at several temperatures (2). Then, either  $F_D$  or  $\phi_D$  (quantum yield which is calculated from  $\tau_D$ ) is used to normalize the efficiency of energy transfer obtained from the quenching at each temperature. The resultant normalized efficiency of energy transfer,  $f$ , is related to both experimental parameters and the donor-acceptor distances as follows.

from time-resolved data:  $f = \langle E \rangle / \langle \phi_D \rangle = C k_t \langle R^{-6} \rangle$

from steady-resolved data:  $f' = \langle E \rangle / \langle F_D \rangle = C' k_t \langle R^{-6} \rangle$ .

Experimental results were obtained by Somogyi in RNase T<sub>1</sub>. Here, a specific Trp is the donor and an acceptor, pyridoxamine phosphate, has been produced by reacting pyridoxal with a Lys side group on the protein. Table I shows a 40% increase in  $f$  between 295 and 320 K, which indicates a 1.85% decrease in  $\langle R \rangle$  as measured by FET.

### Energy Transfer over 42 Å in Human Serum Transferrin

Energy transfer in human serum transferrin from a donor Tb(III) in site B to an Fe(III) acceptor in site A has been used to calculate an intersite distance of  $35.5 \pm 4.5$  Å (3). Previous work that we have done comparing energy transfer in Tb-Tf using either Mn(III) or Fe(III) as an acceptor has shown that this energy transfer depends upon the inverse sixth power of the distance, consistent with a Förster dipole-dipole mechanism. Thus, the energy transfer in this system should be extremely sensitive to changes in  $R$ . Fig. 2 shows recent results from crystallographic data of the overall dimensions of lactoferrin, a structurally homologous protein (4). Fig. 3 shows the thermal profile of Tb(III) donor emission intensity upon direct excitation (502 nm) in the absence (Fig. 3 A), and presence (Fig. 3 B) of Fe(III) acceptor. Förster quenching is apparent by the decrease in the 550-nm donor emission in the presence of Fe(III) (compare intensities in Fig. 3, A vs. B). Analysis of the thermal profile for the experiment is shown in Fig. 7

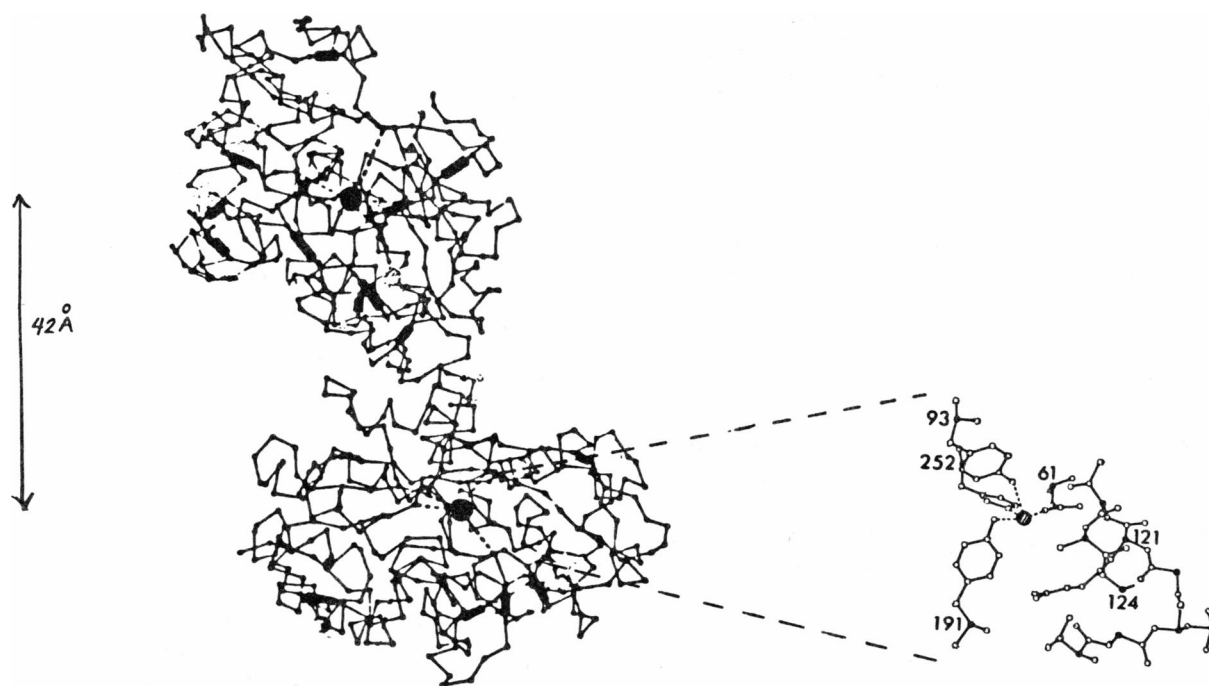


FIGURE 2 A tracing of the  $\alpha$ -carbon backbone of the lactoferrin molecule as interpreted from crystal structure data from reference 4. The two Fe(III) binding sites are 42 Å apart. Shown next to the protein is the structure of the metal ion binding site A, showing the Tyr 93, Tyr 191, His 252, and Asp 61 protein ligands.

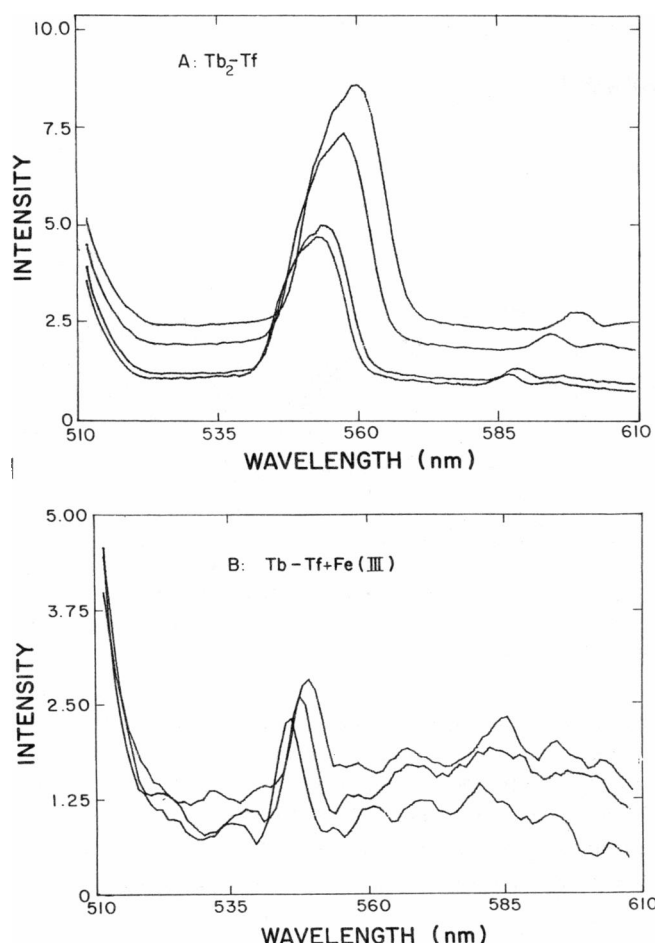


FIGURE 3 Thermal profile of energy transfer from direct excitation of Tb(III) in transferrin. (A) Tb(III) donor in the absence of Fe(III) acceptor and (B) Tb(III) donor in the presence of Fe(III) acceptor between 296 and 319 K. The higher temperature spectra are raised and shifted for presentation purposes. The Tb(III) is directly excited at 502 nm.

and summarized in Table I. For direct excitation, the normalized FET increases 35% between 295 and 320 K. The increase in FET is predicted by the Somogyi model. The magnitude of the increase is compared with that for other proteins in Fig. 7.

#### Energy Transfer over 6.5 Å in Bovine Brain Calmodulin

The  $\alpha$ -carbon backbone of bovine brain calmodulin is shown in Fig. 4 (12). Energy transfer occurs over 6.5 Å from a Tyr 99 to a Tb(III) ion at site IV. This simplified one donor model can be utilized in CaM because the only other possible fluorescent donor is Tyr 138, which has been shown to have its intrinsic fluorescence quenched by its environment (13). The distances of Tyr 99 to the various Ca(II) sites, calculated from crystallographic data, show that Tyr 99 is closest to site IV and thus Tb(III) at site IV would be the predominant acceptor of the donor energy, though site III would contribute somewhat to the energy

transfer. Fig. 4 shows that sites I and II, in the COOH-terminal domain, are separated from Tyr 99 by a 30-Å helix and would therefore not contribute to the quenching.

Fig. 5 shows the thermal profile of the fluorescence intensity of Tyr 99 in the absence (Fig. 5 A) and the presence (Fig. 5 B) of acceptor. Quenching of Tyr fluorescence by the presence of acceptor is apparent. Both systems show a decreased fluorescent intensity with increased temperature. By taking the ratio of the two, it is clear that the FET increases with temperature. Table I reports that the normalized energy transfer parameter  $f$ , increases 40% between 295 and 320 K. The temperature dependence for the normalized FET in CaM is shown in Fig. 7.

#### Temperature Dependence of a Non-Förster Process: Energy Transfer over Very Short Distances in Human Serum Transferrin

Tf contains two metal-binding sites, each of which contains one or two tyrosine residues which contribute to ligation of

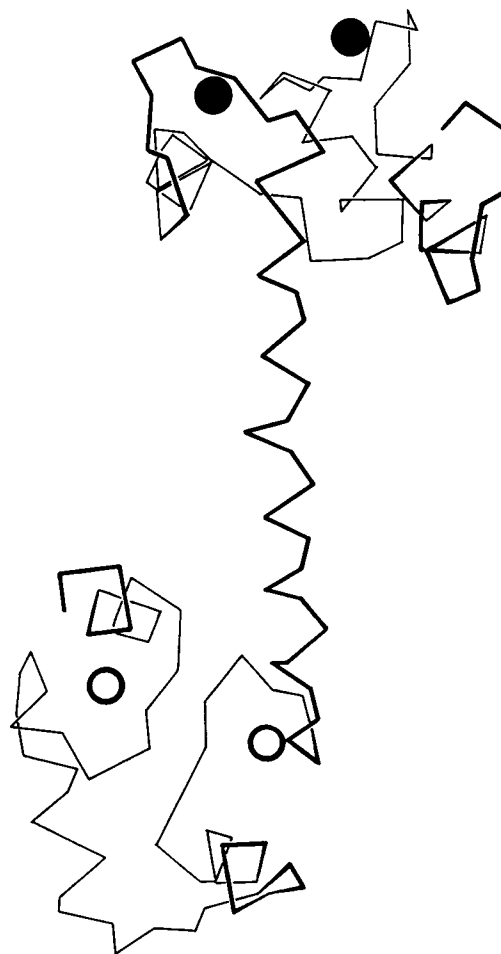


FIGURE 4 The  $\alpha$ -carbon backbone of the calmodulin molecule as interpreted from crystal structure data from reference 12. Ca(II) sites I and II are solid circles and sites III and IV are open circles.

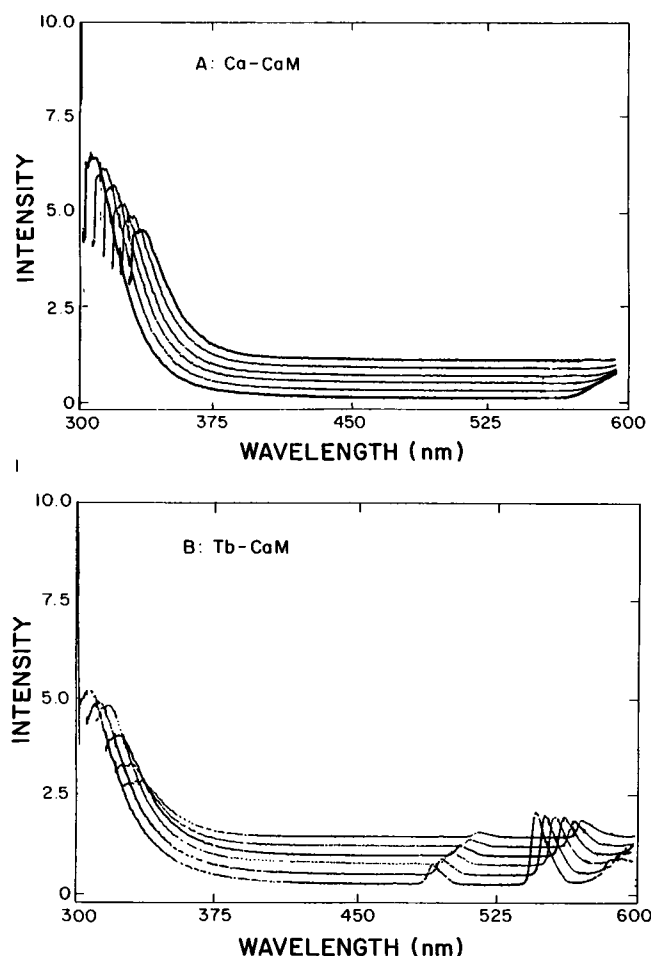


FIGURE 5 Thermal profile of energy transfer from direct excitation of Tyr 99 in calmodulin. (A) Fluorescence from the Tyr donor in the absence of Tb(III) acceptor and (B) fluorescence from the Tyr donor in the presence of Tb(III) acceptor between 283 and 333 K. The higher temperature spectra are raised and shifted for presentation purposes. Tyr is excited directly at 278 nm.

the metal through the phenolic oxygen. The phenomenon of energy transfer from these tyrosine ligands to a chelated Tb(III) cannot be described by Förster's through space dipole-dipole mechanism because the wave functions of the Tyr donor may overlap with the metal acceptor at such short distances. It is impossible to monitor the donor emission directly in this system because the tyrosine is part of a complex aromatic network in which energy migration makes interpretation of the aromatic envelope in the fluorescent emission difficult. Fig. 6 shows the temperature dependence of the Tyr-Tb transfer indirectly by measuring the emission of the Tb(III) acceptor. From 298 K to 323 K the acceptor emission increases 101%. It is obvious from the dramatic increase in the acceptor's emission that the transfer efficiency must also increase with temperature. In fact, the transfer efficiency must increase fast enough to offset thermally activated vibrational deexcitation modes which normally quench Tyr emission at higher temperatures. The implication of this

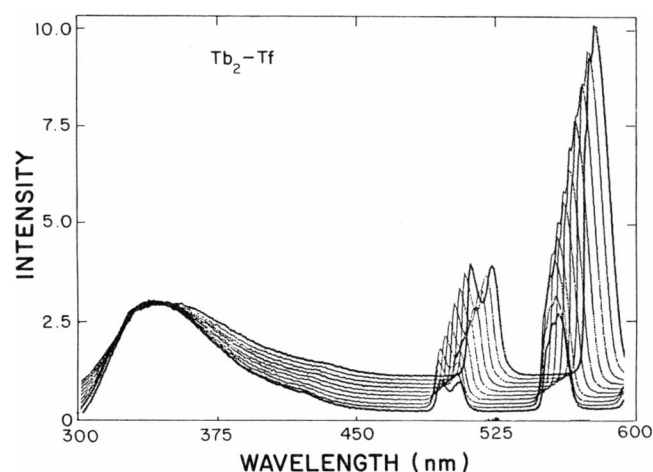


FIGURE 6 Thermal profile of energy transfer from Tyr to Tb(III) in transferrin as monitored by the increase in the acceptor Tb(III) emission. Intrinsic protein fluorescence and luminescence from the Tb(III) acceptor are shown every 5° between 283 and 328 K. The higher temperature spectra are raised and shifted for presentation purposes. Tyr ligands are excited at 295 nm.

result is that processes governing energy transfer at short distances, such as exchange interactions are intrinsically much more temperature-dependent than the dipole-dipole interactions discussed above. This result is consistent with earlier predictions by Dexter of the relative importance of temperature to various energy transfer processes (14).

## DISCUSSION

In general, energy transfer increased as the temperature increased, indicating a decrease in the averaged distance between donor and acceptor. Results for Trp → PMP in RNase, Tyr → Tb(III) in CaM, and Tb(III) → Fe(III) in Tf are summarized in Table I and compared in Fig. 7. In Tf, normalized energy transfer from Tb(III) to Fe(III) increased 35% over a 25° temperature range. Given that the two sites are ~42 Å apart, this represents a 1.81% decrease in the averaged donor-acceptor distance at the higher temperature. Our results predict a rather rigid global Tf structure within the millisecond lifetime of the Tb(III) donor. Thus, hinge bending modes, which have been postulated to occur in Tf and which would be expected to greatly decrease the intersite distance for this protein, were not observed in this experiment. In CaM, normalized energy transfer from Tyr to Tb(III) in CaM increased 40% over the same temperature range for a 1.85% decrease in the averaged donor-acceptor distance. Assuming that the Tyr to Tb(III) distance is the same as Tyr to Ca(II), this represents a change in the averaged distance as measured from FET from 6.50 to 6.38 Å at the higher temperature. Thus there is limited flexibility in the COOH-terminal domain within the Tyr excited state lifetime. Almost identical behavior was observed for RNase by Somogyi (40% increase over 25°). In summary, energy transfer varied from 35% in Tf to 40% in CaM and

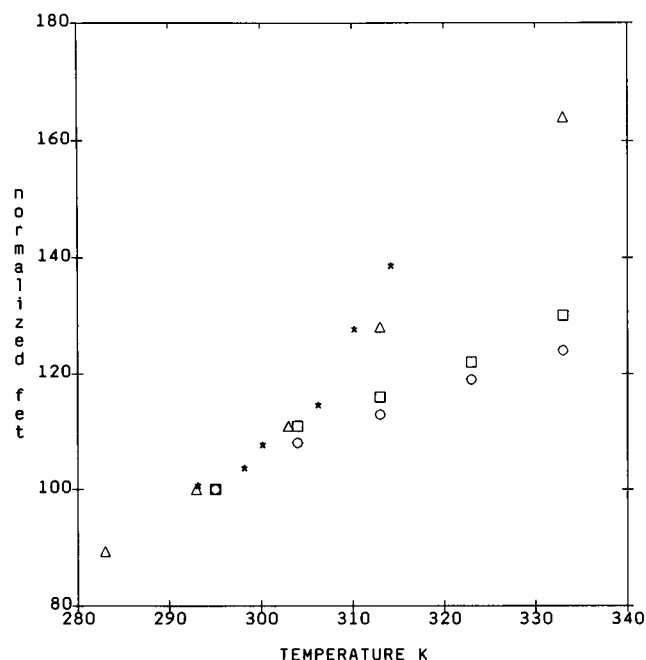


FIGURE 7 Temperature dependence of the normalized energy transfer for three different protein systems: (\*) Trp to pyridoxamine monophosphate in RNase from reference 2; (Δ), Tyr to Tb(III) in calmodulin; and (□ and ○) energy transfer from Tb(III) to Fe(III) under conditions of buffer A and buffer B, respectively.

RNase over the same temperature range. It is not yet clear whether this implies that the technique is proving insensitive to protein structure or whether the proteins that we have chosen happen to have similar flexibilities.

The dynamic aspect of biomolecules in solution has recently come under close scrutiny (15, 16). Both local and global motions may be fundamental to an understanding of a range of biological functions from substrate binding to ion transport. The range of time scales for these biochemical fluctuations is quite broad;  $10^{-14}$  s for small-scale local motions to  $10^2$  s for rare structural or global transitions. Despite rapid advances in the simulation of protein dynamics (17), experimental measurements of these events has been difficult. Several groups have proposed experimental approaches which utilize spectroscopic methods to investigate protein motions (2, 18–21). This investigation has shown that the thermal profile of energy transfer can be used to probe fluctuations in a protein matrix as previously suggested (2), however, it is not yet clear whether the technique is sensitive enough to differences in the protein host matrices to make it structurally useful. Further investigations into other donor-acceptor environments should lend clearer insight into the generality and usefulness of this technique.

We gratefully acknowledge the generosity of Prof. E. N. Baker for making lactoferrin protein coordinates available to us. Calmodulin coordinates were obtained from the Brookhaven Data Bank.

This work was supported by the Research Corporation, The Petroleum Research Fund, and National Science Foundation Grant DMB 8600814. Summer salary for M.R. was generously donated by E. I. Dupont de Nemours & Co.

Received for publication 15 June 1987 and in final form 19 Jan 1988.

## REFERENCES

1. Stryer, L. 1978. Fluorescence energy transfer as a spectroscopic ruler. *Annu. Rev. Biochem.* 47:819–846.
2. Somogyi, B., J. Matko, S. Papp, J. Hevessey, G. R. Welch, and S. Damjanovich. 1984. Förster-type energy transfer as a probe for changes in local fluctuations of protein matrix. *Biochemistry* 23:3403–3411.
3. O'Hara, P. B., S. M. Yeh, C. F. Meares, and R. Bersohn. 1981. Distance between metal-binding sites in transferrin: energy transfer from bound terbium(III) to iron(III) or manganese(III). *Biochemistry* 20:4704–4708.
4. Anderson, B. F., H. M. Baker, E. J. Dodson, G. E. Norris, S. V. Rumball, J. M. Waters, E. N. Baker. Structure of human lactoferrin at 3.2 Å resolution. *Proc. Natl. Acad. Sci. USA* 84:1769–1773.
5. Kretsinger, R. H., S. E. Rudnick, and L. J. Weissman. 1986. Crystal structure of calmodulin. *J. Inorg. Biochem.* 28:289–302.
6. Aisen, P., and I. Listowsky. 1980. Transferrin and the siderophilins. *Annu. Rev. Biochem.* 49:357–393.
7. O'Hara, P. B., and S. H. Koenig. 1986. Electron spin resonance and magnetic relaxation studies of gadolinium(III) complexes with human transferrin. *Biochemistry* 23:1445–1450.
8. Harris, D. C. 1977. Proteins of Iron Metabolism. W. D. Brown, editor. Grune & Stratton Inc., New York. 197–217.
9. Gopalakrishna, R., and W. B. Anderson. 1982. Ca(II)-induced hydrophobic site on calmodulin: application for purification of calmodulin by phenyl-Sepharose affinity chromatography. *Biochem. Biophys. Res. Commun.* 104:830–836.
10. Dedman, J. R., and A. R. Means. 1977. Characterization of a spectrophotometric assay for cAMP phosphodiesterase. *J. Cyclic Nucleotide Protein Phosphorylation Res.* 3:139–152.
11. Förster, T. 1948. Intermolecular energy migration and fluorescence. *Annalen der Physik* 2:55–75.
12. Babu, Y. S., J. S. Sack, T. J. Greenhough, C. E. Bugg, A. R. Means, and W. J. Cook. 1985. Three-dimensional structure of calmodulin. *Nature (Lond.)* 315:37–40.
13. Kilhoffer, M. C., J. G. Demaille, and D. Gerard. Tyrosine fluorescence of ram testis and octopus calmodulins. Effects of calcium, magnesium, and ionic strength. *Biochemistry* 20:4407–4414.
14. Dexter, D. L. 1953. A theory of sensitized luminescence in solids. *J. Chem. Phys.* 21:836–850.
15. McCammon, J. A., and M. Karplus. 1980. Simulation of protein dynamics. *Annu. Rev. Phys. Chem.* 31:29–45.
16. Karplus, M., and J. A. McCammon. 1981. The internal dynamics of globular proteins. *CRC Crit. Rev. Biochem.* 9:292–349.
17. Elber, R., and M. Karplus. 1987. Multiple conformational states of proteins: a molecular dynamics analysis of myoglobin. *Science (Wash. DC)* 235:318–321.
18. Haas, E., and I. Z. Steinberg. 1984. Intramolecular dynamics of chain molecules monitored by fluctuations in efficiency of excitation energy transfer, a theoretical study. *Biophys. J.* 46:429–437.
19. Cross, A. J., and G. R. Fleming. 1986. Influence of inhibitor binding on the internal motions of lysozyme. *Biophys. J.* 50:507–519.
20. Xu, G. J., and G. Weber. 1982. Dynamics and time-averaged chemical potential of proteins: importance of oligomer association. *Proc. Natl. Acad. Sci. USA* 79:5268–5271.
21. Demchenko, A. P. 1986. Fluorescence analysis of protein dynamics. *Essays Biochem.* 22:120–157.